Concentration dependence of the wave vector of the spin-density wave of chromium alloys

K. Schwartzman

Department of Physics, Indiana University of Pennsylvania, Indiana, Pennsylvania 15705

J. L. Fry and Y. Z. Zhao

Department of Physics, University of Texas at Arlington, Arlington, Texas 76019

(Received 24 October 1988)

The static, unenhanced paramagnetic susceptibility of pure Cr and its dilute alloys with V and Mn is computed within the random-phase approximation at zero temperature. Matrix elements are calculated using a linear-combination-of-atomic orbitals scheme and alloying is treated by both the rigid-band and coherent-potential approximations. The susceptibility exhibits peaks at wave vectors which correlate well with Fermi-surface nesting features and which are indicative of antiferromagnetic instabilities leading to spin-density-wave ground states. These wave vectors agree to within 1% with neutron scattering measurements of the spin-density-wave wave vector in pure Cr, and the calculated dependence of this wave vector on V or Mn impurity concentration follows experimental variations closely. The unenhanced paramagnetic susceptibility of pure Mo is computed as well; and the absence of a spin-density wave, despite strong similarities between the Fermi surfaces of Cr and Mo, is attributed to matrix-element behavior and exchange and correlation corrections.

I. INTRODUCTION

There has been considerable interest in the antiferromagnetism of Cr and its alloys for some time. This is largely a result of the fact that Cr is the only element known to have a spin-density-wave (SDW) ground state. The SDW is slightly incommensurate with the lattice, and it has a wave vector $q_{SDW} = 0.96(2\pi/a)$ in the [100] direction as observed in neutron scattering experiments.[1]

The appearance of an SDW arises from a complex interplay of Fermi-surface nesting, electronic exchange[2] and correlation,[3] and matrix-element effects. In pure Cr it has been recognized[4] for twenty-five years that two branches of the Fermi surface (the electron jack at Γ and the hole octahedron at H) exhibit significant nesting at the wave vector for which the observed SDW is found. Consequently, one may infer that nesting is an important mechanism for the SDW in Cr. This point shall be reemphasized in Sec. IV based on the results of the current study.

While Fermi-surface nesting may very well be a necessary condition for the appearance of an SDW in Cr it is surely not sufficient. This conclusion can be drawn from several observations. First, such nesting is also associated with instabilities leading to charge-density waves. Secondly, the Fermi surfaces of Mo and W also exhibit nesting features, yet neither of these metals has been observed to exhibit an SDW. As discussed in Sec. IV, the behavior of the transition matrix elements in the case of Mo suppresses the SDW, and it may be presumed that the same mechanism is responsible for the absence of an SDW in W.

Electronic exchange and many-body effects must also play a role in the appearance of an SDW. On the one hand, Coulomb renormalization of band energies and matrix elements must be accounted for, although this can cause only small quantitative changes in predictions made using the corresponding bare-electron quantities. Furthermore, it is well known that the Pauli paramagnetic susceptibility is unaffected by the electron-phonon interaction. On the other hand, however, exchange and correlation effects on the polarization bubble can be responsible for qualitative changes in the susceptibility. In principle, the full wave-vector dependence of the susceptibility is affected and the SDW wave vector can be substantially shifted. Such enhancement could lead to an SDW in systems where Fermi-surface nesting is not as significant as in Cr, or conspire with matrix elements effects to suppress an SDW where nesting is significant (such as in Mo).

In this paper a detailed examination is made of the random-phase-approximation (RPA) paramagnetic spin susceptibility of Cr and its alloys with Mn and V, and of pure Mo. The unenhanced susceptibility within the RPA is calculated from first principles at zero temperature as a function of wave vector. Since the calculation is done in the paramagnetic phase, sharp peaks or poles in the susceptibility can be interpreted as an antiferromagnetic instability leading to the SDW. Finding the wave vector of the SDW in this way leads to good agreement with experimental data for Cr and its dilute alloys.

The outline of this paper is as follows. In Sec. II the theoretical formulation of the paramagnetic susceptibility and its ingredients is presented. The computational method used in evaluating the susceptibility is discussed in Sec. III and the results of the calculation are given in Sec. IV, where comparison is made with experimental measurements. The conclusions drawn from the present investigation are discussed in Sec. V.

II. THEORETICAL FORMULATION

A direct approach to this problem would be to perform antiferromagnetic total-energy and band-structure calculations from the outset. Difficulties in such a procedure have already been pointed out,[5] and a calculation of this type is not attempted here. An excellent, comprehensive review of both theoretical and experimental studies of the magnetic properties of chromium was published in 1988 by Fawcett,[6] so it is not the intention here to review the numerous theoretical papers. These papers fall into two categories: (1) model studies incorporating the incommensurate spin-density-wave structure and (2) first-principles studies based upon the paramagnetic or commensurate antiferromagnetic structure. Several papers in the first-principles category are relevant to the present approach and should be mentioned, although they did not consider explicitly any of the alloys of chromium treated here.

Gupta and Sinha[7] made the first serious attempt to compute the wave-vector-dependent susceptibility $\chi(\mathbf{q})$, but used non-self-consistent band-structure and numerical-integration procedures which are not up to today's standards. Windsor did a similar calculation and furthermore included many-body enhancements with a parametrized Stoner-like theory.[8] Both authors identified correctly the importance of interband and intraband contributions to the susceptibility, but could not compute accurately the wave vector of the spin-density wave.

On the other hand Skriver[9] and Kubler[10] performed first-principles studies for an assumed commensurate form of antiferromagnetic chromium using more-accurate band-theory techniques and modern local-density theory. Skriver performed band calculations and constructed an accurate Stoner-like theory of antiferromagnetism. He also warned about the possible sensitivity of conclusions to the particular choice of density functional employed in the calculations. Kubler minimized the total energy of the commensurate structure and showed that it was more stable than the paramagnetic or ferromagnetic phases. He obtained a value for the magnetic moment which compared well with the experimental (incommensurate) moment. While both these studies were satisfying in that they supported an antiferromagnetic state for chromium, neither approach was able to explain the actual incommensurate structure of the spin-density wave found experimentally in chromium and some of its alloys.

In order to study the SDW in Cr and its alloys, in this paper the paramagnetic susceptibility is examined for an instability towards the antiferromagnetic phase. Such an instability will be manifested by a divergence in the susceptibility at a wave vector $\mathbf{q}_{SDW}$ where the SDW could be observed (as in a neutron scattering experiment, for example). If the divergence in the paramagnetic susceptibility at $\mathbf{q}_{SDW}$ is "smooth", then the transition to the antiferromagnetic state would be expected to be second order. The present work, as well as a previous calculation of the susceptibility,[7] finds behavior of this type, although observation of logarithmic singularities with numerical calculations is very difficult. Experimental evidence suggests the transition is first order (or, at least, "nearly"

first order).[6] It is apparent, as has been pointed out earlier,[7] that the physical system in question cannot be quantitatively described by paramagnetic theory in the vicinity of the transition. It should not be surprising then that the order of the transition may not be accurately predicted using the present approach (see Ref. 11 for an alternative reason). On the other hand, the wave vector of the SDW can be determined accurately since it is the wave vector at which a divergence does occur in the paramagnetic susceptibility.

The philosophy adopted in the present study is one which leads to a detailed understanding of the properties of real systems within the RPA. This has the inherent shortcoming of neglecting short-ranged correlations in the (long-ranged) RPA screened Coulomb interaction (i.e., approximating the Coulomb vertex by unity). However, these correlations may often be approximately separated from the long-ranged contribution. In this way, expressions of the generalized Stoner-type can be obtained for the enhanced susceptibility

$$\chi(\mathbf{q}) = \frac{\chi^0(\mathbf{q})}{1 - I(\mathbf{q})\chi^0(\mathbf{q})} \ , \tag{1}$$

where $\chi^0(\mathbf{q})$ is the RPA susceptibility and $I(\mathbf{q})$ is an enhancement factor containing the short-ranged correlations.

Strictly speaking, the susceptibility in Eq. (1) diverges only when the denominator vanishes [apart from a fortuitous case in which $I(\mathbf{q})$ is zero for the wave vector at which the RPA susceptibility diverges]. This divergence is a consequence of the interplay of the short-ranged interactions embodied in $I(\mathbf{q})$ and the "uncorrelated", screened Coulomb interaction arising in the RPA. Such a situation is reminiscent of the ferromagnetic instability which arises from the behavior of $I(0)$ and $\chi^0(0)$.

In the limit that short-ranged correlations are neglected it becomes necessary to investigate the divergent behavior of the RPA susceptibility. Even when they are considered, a divergence in the full susceptibility can generally be expected when $\chi^0(\mathbf{q})$ diverges (or has a sharp maximum). This conclusion can be drawn from the work of Janak[12] who finds a smooth variation in $I(\mathbf{q}=0)$ as a function of atomic number for the metals V, Cr, and Mn. Since neither V nor Mn exhibit magnetic behavior and both $\chi^0(0)$ and $I(0)$ are small for Cr, the SDW in Cr is expected to arise primarily from single-particle properties, namely, Fermi-surface nesting, or from a strong variation of $I(q)$ with q. The role played by $I(q)$ in the susceptibility will be examined in detail in a future paper. For the remainder of the present study the paramagnetic susceptibility within the RPA will be considered.

The frequency-independent RPA susceptibility is

$$\chi^0(\mathbf{q}) = -2\mu_0\mu_B^2 \sum_{\mathbf{k},\mu,\mu'} \frac{|M_{\mu\mu'}(\mathbf{k},\mathbf{k}+\mathbf{q})|^2}{E_{\mathbf{k}\mu} - E_{\mathbf{k}+\mathbf{q}\mu'}} (f_{\mathbf{k}\mu} - f_{\mathbf{k}+\mathbf{q}\mu'}) \ , \tag{2}$$

where $E_{\mathbf{k}\mu}$ is the band energy for wave vector $\mathbf{k}$ and band index μ, $f_{\mathbf{k}\mu}$ is the equilibrium Fermi occupation factor for this energy, μ_B is the Bohr magneton, and μ_0 is the magnetic permeability of the vacuum. When there is

nesting of branches of the Fermi surface for a wave vector $\mathbf{q}$, the energy denominator in Eq. (2) becomes small. Consequently, if sufficient areas of the Fermi-surface nest, the susceptibility can show strong peaking, indicative of an antiferromagnetic instability. The behavior of the matrix elements connecting $\mathbf{k}\mu$ and $\mathbf{k}+\mathbf{q}\mu'$ modify nesting effects, and may be expected to either sharpen or weaken a tendency toward instability.

The form of the matrix elements employed here is based on the work of Callaway et al.[3] who originally developed the approach for application to ferromagnetic metals. The matrix elements are written as

$$M_{\mu\mu'}(\mathbf{k},\mathbf{k}+\mathbf{q})=\sum_{mn} A_{m\mu}^{+}(\mathbf{k})I_{mn}(\mathbf{q})A_{n\mu'}(\mathbf{k}+\mathbf{q}) , \quad (3)$$

where $A_\mu(\mathbf{k})$ is the eigenvector of a band Hamiltonian for wave vector $\mathbf{k}$ and band μ, and $I_{mn}(\mathbf{q})$ is a form-factor matrix element for the neutral atom. In practice, the eigenvectors are obtained from a Slater-Koster fit to a first-principles band structure as discussed in Sec. III. The essential assumption which dictates the form of Eq. (3) is that the overlap between the d orbitals on neighboring atomic sites can be neglected. The form factor is written[3]

$$I_{ij}(\mathbf{q})=\delta_{ij}I^{(0)}(q)-5I^{(2)}(q)c_{ij}^{(2)}(\hat{\mathbf{q}})$$
$$+9I^{(4)}(q)c_{ij}^{(4)}(\hat{\mathbf{q}}) , \quad (4)$$

where $\hat{\mathbf{q}}$ is the unit vector in the direction $\mathbf{q}$ and the c_{ij} are polynomials tabulated in Ref. 3. The superscripts in Eq. (4) indicate the appropriate orbital angular momentum quantum number and the $I^{(l)}(q)$ are the radial integrals which for $3d$ metals are

$$I^{(l)}(q)=\int_0^\infty r^2 R^2(r)j_l(qr)dr , \quad (5)$$

where the $R(r)$ are Clementi wave functions for the d states of the neutral atom

$$R(r)=\sum_j \alpha_j r^2 e^{-\rho_j r} . \quad (6)$$

The quantities α_j and ρ_j are tabulated parameters.[13] Equation (5) can now be integrated analytically, resulting in an algebraic expression for the form factor. Full details of the evaluation of the form factor are given in Ref. 3.

In order to treat alloying within this framework, the rigid-band approximation can be employed. This assumes that atoms of the impurity species only serve as donors or acceptors of electrons. The electron density and Fermi energy are altered, but the underlying band structure of the host metal is not affected. Since atomic wave functions appear in the form factor, the latter must be modified to accommodate alloying. This is done by assuming that the impurity atoms contribute to the alloy form factor proportionally to their concentration with the host atoms making up the balance. For example, for $Cr_{1-x}V_x$ alloys the form factor is approximated by

$$I_{ij}^{Cr_{1-x}V_x}(\mathbf{q})=xI_{ij}^{V}(\mathbf{q})+(1-x)I_{ij}^{Cr}(\mathbf{q}) , \quad (7)$$

where x is the impurity concentration.

For the present study, a Slater-Koster version of the coherent-potential approximation (CPA) is used.[14] In this treatment, an averaged lattice constant for the alloy $A_{1-x}B_x$ is defined by

$$a=(1-x)a_A+xa_B , \quad (8)$$

where a_A and a_B are the lattice constants of the pure metals A and B, respectively. The bond parameters for the alloy may then be found by application of the Harrison scaling scheme.[15] In an obvious notation, the alloy bond parameters are written

$$V_{A_{1-x}B_x}=(1-x)\left[\frac{a_A}{a}\right]^n V_A+x\left[\frac{a_B}{a}\right]^n V_B , \quad (9)$$

where n is -2 for s—s, s—p, and p—p bonds, $-\frac{7}{2}$ for s—d and p—d bonds, and -5 for d—d bonds. These parameters are then used to generate the alloy band structure. The only remaining quantity in the susceptibility to contend with in modeling alloys is the form factor which is treated the same as in the rigid-band approximation above, Eq. (7).

III. COMPUTATIONAL SCHEME

As a first step in reducing the susceptibility [Eq. (2)] to a form convenient for numerical calculation, the wave-vector sum is restricted to an irreducible $\frac{1}{48}$ of the Brillouin zone (IBZ). In this way

$$\chi^0(\mathbf{q})=-2\mu_0\mu_B^2 \sum_\beta \sum_{\mu,\mu'} \sum_{\mathbf{k}_i \in IBZ} \frac{|M_{\mu\mu'}(\hat{\beta}\mathbf{k}_i,\hat{\beta}\mathbf{k}_i+\mathbf{q})|^2}{E_{\hat{\beta}\mathbf{k}_i\mu}-E_{\hat{\beta}\mathbf{k}_i+\mathbf{q}\mu'}}$$
$$\times(f_{\hat{\beta}\mathbf{k}_i\mu}-f_{\hat{\beta}\mathbf{k}_i+\mathbf{q}\mu'}) , \quad (10)$$

where the $\mathbf{k}_i$ are restricted to the IBZ and the $\hat{\beta}$ sum runs through the 48 rotation operators which map the IBZ into the full first zone. An immediate simplification arises since the band energies are invariant under rotation to an equivalent point in the zone

$$E_{\hat{\beta}\mathbf{k}_i\mu}=E_{\mathbf{k}_i\mu} , \quad (11a)$$

$$E_{\hat{\beta}\mathbf{k}_i+\mathbf{q}\mu'}=E_{\mathbf{k}_i+\hat{\beta}^{-1}\mathbf{q}\mu'} . \quad (11b)$$

Since the occupation factors depend only on energy, it remains only to consider the role of the $\hat{\beta}$ rotations in the matrix elements. The eigenvectors transform under rotation according to

$$A(\hat{\beta}\mathbf{k}_i)=\hat{\beta}A(\mathbf{k}_i) , \quad (12)$$

so that the matrix elements appearing in Eq. (10) may be written

$$M_{\mu\mu'}(\hat{\beta}\mathbf{k}_i,\hat{\beta}\mathbf{k}_i+\mathbf{q})=\sum_{m,n} [\hat{\beta}A_\mu^\dagger(\mathbf{k}_i)]_m I_{mn}(\mathbf{q})$$
$$\times[\hat{\beta}A_{\mu'}(\mathbf{k}_i+\hat{\beta}^{-1}\mathbf{q})]_n . \quad (13)$$

Consequently the susceptibility takes the form

$$\chi^0(\mathbf{q}) = -2\mu_0\mu_B^2 \sum_{\beta} \sum_{\mu,\mu'} \sum_{\mathbf{k}_i \in \mathrm{IBZ}} \frac{|M_{\mu\mu'}(\hat{\beta}\mathbf{k}_i, \hat{\beta}\mathbf{k}_i + \mathbf{q})|^2}{E_{\mathbf{k}_i\mu} - E_{\mathbf{k}_i+\mathbf{q}'\mu'}}$$

$$\times (f_{\mathbf{k}_i\mu} - f_{\mathbf{k}_i+\mathbf{q}'\mu'}) \ ,$$

(14)

where $\mathbf{q}' = \hat{\beta}^{-1}\mathbf{q}$ and the matrix elements are written out in Eq. (13).

In Eq. (14), the rotation operators $\hat{\beta}$ appear generally in the role of transforming $\mathbf{q}$. Depending on the symmetry of $\mathbf{q}$, not all of the 48 rotations yield a unique vector. In particular, there are only 6 distinct rotations for $\mathbf{q} \propto (1,0,0)$, 8 for $\mathbf{q} \propto (1,1,1)$, and 12 for $\mathbf{q} \propto (1,1,0)$. Since the symmetry directions are generally of the most interest, this yields a further simplification which significantly reduces computing times. The primary reduction results from the fact that the band structure, $E_{\mathbf{k}_i+\mathbf{q}'\mu'}$ and $A_{\mu'}(\mathbf{k}_i + \mathbf{q}')$, need only be found for the distinct $\mathbf{q}'$. The $\hat{\beta}$ rotations of the eigenvectors in calculating the matrix elements do not constitute a substantial expense of time.

As a matter of convenience, and to gain an additional savings of computing time, the band structure is obtained from a 34-parameter Slater-Koster fit[16] to a first-principles linear-combination-of-atomic-orbitals (LCAO) calculation for Cr.[17] Since the details of the calculation and fitting procedure are discussed elsewhere[16] it suffices to indicate here that the fit has a rms error of less than 0.3 mRy. As is appropriate for a transition metal such as Cr, 9 bands (and basis vectors)—1s, 3p, and 5d—must be summed over in an expression such as Eq. (13).

In order to find the matrix elements it is necessary to evaluate the form factor $I_{ij}(\mathbf{q})$; note that this quantity need only be calculated once for each $\mathbf{q}$. As indicated in Sec. II, the formulation by Callaway et al.[3] for I_{ij} is appropriate only for the d basis vectors, and these are approximated by the neutral atom wave functions of Clementi and Roetti.[13] For the calculation to remain tractable, the s and p contributions to the form factor are treated as plane waves in the Born approximation. This is equivalent to setting the s and p parts to a Kronecker δ function and ignoring s-d and p-d mixing.

The wave-vector sum in Eq. (14) is performed using the analytic tetrahedron method (ATM).[18] In this approach, the IBZ is decomposed into a integral number of non-overlapping tetrahedra, each of whose four vertices lies at the tip of one if the $\mathbf{k}_i$ participating in the wave-vector sum. Three sets of $\mathbf{k}_i$ are used in this calculation generated from 8, 20, or 24 equal divisions along the Δ line. These correspond, respectively, to 55, 506, and 819 $\mathbf{k}_i$ points in the IBZ.

For a tetrahedron defined by four wave vectors $\mathbf{k}_j$ to contribute to the susceptibility, it must contain at least some occupied states in the band μ, and the corresponding tetrahedron defined by $\mathbf{k}_j + \mathbf{q}$ must contain some unoccupied states in the band μ'. If a branch of the Fermi surface passes through a tetrahedron, the surface element is assumed to be a plane. In the limit of sufficient $\mathbf{k}_i$ point density, this becomes a reasonable approximation. The Fermi wave vectors within a tetrahedron through which the Fermi surface passes are determined by interpolation between the band energies at the vertices and the Fermi energy; the latter quantity is found from an independent density-of-states calculation. The two sections of the tetrahedron separated by the Fermi surface are subdivided into smaller tetrahedra with the matrix elements at the vertices determined by interpolation. This is generally preferable to constant matrix-element schemes employed by earlier workers[7] since it improves the accuracy of the computed susceptibility using a relatively modest number of wave vectors $\mathbf{k}_i$ in the IBZ.

Results for the susceptibility presented in Sec. IV are calculated using 506 $\mathbf{k}_i$ points in the IBZ. Comparison with calculations along the major symmetry directions using 819 $\mathbf{k}_i$ points yields agreement to within one percent of the 506-point calculations, and it may be concluded that the mesh density used here provides accurate results for the susceptibility within the theoretical formulation described earlier.

IV. RESULTS

In order to gain insight into the role of Fermi-surface geometry in producing the SDW in Cr, it is useful to consider a calculation of the paramagnetic susceptibility in which the matrix elements are taken to be unity. This permits matrix element behavior to be partially distinguished from nesting effects, clarifying the physical origins of the SDW. The results of this calculation are shown in Fig. 1. As may be seen, there is significant variation of this "unnormalized" susceptibility over the zone. In particular, a well-defined peak appears at the nesting wave vector which, as previously discussed, corresponds to the observed SDW wave vector. This is strongly suggestive of a connection between the two, but several problems with Fig. 1 should be pointed out. First, the peak (pole?) sharpness is hard to estimate. Second, there are other maxima present, including that at $\mathbf{q}=0$. Third, the
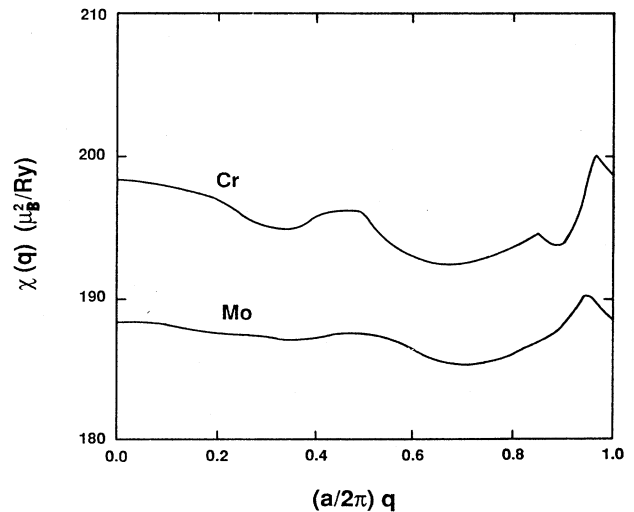

FIG. 1. RPA susceptibility for Cr and Mo along the Δ line in the bcc Brillouin zone using matrix elements of unity.

q→0 limit is wrong by an order of magnitude because of the failure to include matrix elements.

Since the Fermi surface of Mo is very similar to that of Cr, one may infer that the unnormalized paramagnetic susceptibilities of the two metals are also similar. This point is established in Fig. 1 where a peak appears at the nesting wave vector of Mo. On the other hand, however, an SDW (or other magnetic instability) has not been observed in Mo. For this absence to be fully understood, it becomes necessary to include matrix elements, as well as exchange and correlation enhancement, in a calculation of the susceptibility.

The computed susceptibility using the matrix elements discussed in Sec. II is shown in Fig. 2 for pure Cr and Mo. In both cases the q→0 limit correctly recovers the density of states at the Fermi surface as found in a separate calculation. Both also exhibit broad maxima in the vicinity of π/a along the Δ line. These maxima arise from the interband matrix elements which increase rapidly with q, while intraband matrix elements rapidly decrease with q. While enhancement corrections will be examined in detail in a future publication, preliminary results[19] indicate that these remove the broad maxima.

The principal feature seen in Fig. 2 is the peak persisting in Cr at the nesting wave vector: Matrix-element variation does not alter q_{SDW}. Moreover, it reinforces the suggestion that Fermi-surface geometry plays a leading role in the formation of the SDW. In the case of Mo, however, the peak in the susceptibility at the nesting wave vector is reduced, suggesting that matrix elements may eliminate the sharp feature. The "sharpness" of these peaks is difficult to determine accurately, and whether there is a logarithmic singularity at q_{SDW} for the true band structures with an exact calculation of $\chi(q)$ may only be surmised. Numerical calculation of the Hartree-Fock density of states for the uniform electron gas is unable to produce the known logarithmic depen-
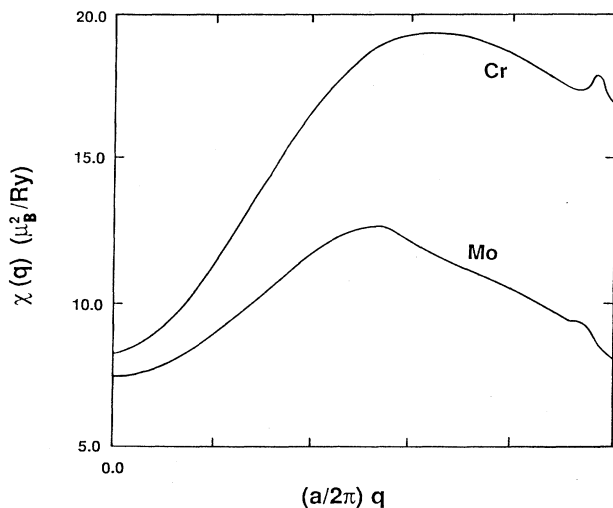
dence using the ATM with a very large number of tetrahedra.[20]

The results discussed above for the paramagnetic susceptibility of Cr agree qualitatively with a previous study of the problem reported by Gupta and Sinha.[7] Their prediction for the wave vector of the SDW, $0.88(2\pi/a)$ along the Δ line, was based on arguments similar to those here since their susceptibility did not exhibit a divergence either. The discrepancy with our value, and the experimental one, is apparently due to differences in bandstructure and matrix elements, and the use of a less accurate integration method than that employed here to compute $\chi^0(q)$.

At this stage it is worth emphasizing a few of the points made above. For one thing, the SDW in Cr is inferred to exist at a wave vector where there may not be true divergence in the susceptibility. Secondly, the wave-vector dependence of the exchange and correlation enhancement could lead to changes in the structure and position in the zone of the SDW. In the first case, there is structure in the portions of the Fermi surface where nesting occurs. In addition, the energy denominator in the susceptibility is small in these regions. Thus, while an accurate calculation of unenhanced susceptibility has been achieved, numerical error can possibly be responsible for suppressing the very fine features associated with the nesting which lead to divergent behavior is $\chi^0(q)$. On this basis, and the sharpness of the peak which is found, it may be concluded the SDW does indeed appear at the wave vector of this peak. In addition, the wave vector of the peak agrees closely with the wave vector of the SDW found experimentally. This lends support to the notion that single-particle effects (nesting and matrix-element variation) are primarily responsible for determining the wave vector of the SDW in Cr. For pure Cr, many-body enhancements have been included in the calculation of $\chi(q)$, resulting in a slight shift in the location of q_{SDW} and producing almost exact agreement with the experimentally observed value. In addition, the enhanced $\chi(q)$ shows a pole instead of a peak at q_{SDW}.[19]

Alloys of Cr with V and Mn also exhibit spin-density waves. The neutron scattering data of Koehler et al.[1] indicate that q_{SDW} increases with increasing concentration of Mn and decreases with increasing concentration of V. By modeling dilute alloys within the rigid-band or CPA approximation the present calculation is able to account for this behavior very well. Results are shown in Fig. 3 and are listed in Table I. Not only are the trends in the data followed closely, but the quantitative agreement is very good as well. The CPA and rigid-band results are essentially the same at these alloy concentrations, so only CPA values are shown in Fig. 3.

Figure 3 includes the low-temperature data of Ref. 1, which is only slightly lower than the high-temperature data reported there. For pure chromium the many-body enhanced susceptibility[19] displays a pole at $q=0.95$ $(2\pi/a)$, yielding almost exact agreement with the data in Fig. 3 at $x=0$. The enhanced susceptibility is much more difficult to compute for the alloys and has not yet been obtained. Assuming that the same small shift in q_{SDW} occurs when enhancement of $\chi^0(q)$ is done for the

FIG. 2. Same as Fig. 1, except the properly normalized wave-vector-dependent matrix elements discussed in the text were employed.
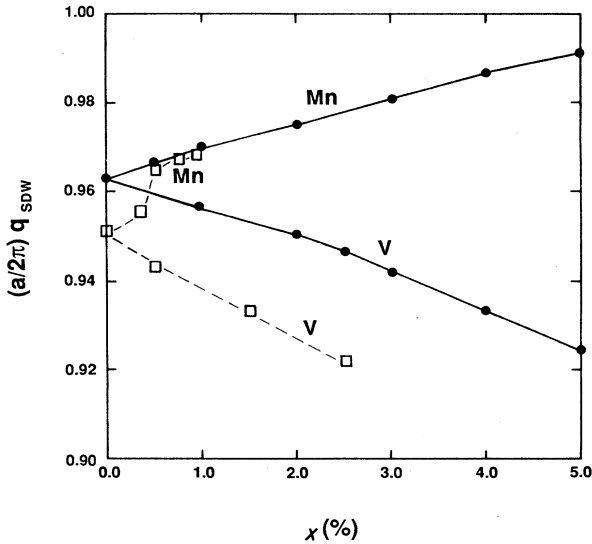
FIG. 3. Concentration dependence of the wave vector of the spin-density wave in alloys of Cr with V and Mn. The origin of the q axis on the graph has been chosen to exaggerate differences between theory and experiment. Squares connected by dashed lines represent the experimental values of Ref. 1 of the text. Solid dots connected by lines are the RPA computed values. x is the concentration of V (Mn) in percent.

TABLE I. Peak positions, q_{SDW} of $\chi^0(q)$ for $Cr_{1-x}(V,Mn)_x$ alloys. Here q_{SDW} is along the Δ axis and is given in units of $(2\pi/a)$, where a is the lattice constant for the alloy.

x	q_{SDW} V	q_{SDW} Mn
0.00	0.9635	0.9635
0.01	0.9565	0.9695
0.02	0.9495	0.9755
0.03	0.9425	0.9815
0.04	0.9330	0.9863
0.05	0.9245	0.9910
0.06	0.9165	0.9950
0.07	0.9080	0.9995

alloys, the values of q_{SDW} in Table I and Fig. 3 would be lowered by about $0.01(2\pi/a)$, and the estimated difference between theory and experiment for Mn and V alloys would be about 1%. Agreement to within this small difference provides further evidence of the strong relationship between the Fermi-surface features of Cr and the wave vector of the associated spin-density wave as originally postulated by Lomer.[4] Note that the spin-density wave is predicted to be commensurate with the lattice in Mn alloys of about 7 at. % (Table I).

A further check of the calculated values is provided by the recent work of Fawcett et al.[21] in which the wave vector of an incommensurate spin-density-wave paramagnon was determined from inelastic neutron scattering in $Cr_{0.95}V_{0.05}$. Their high-temperature result is $q = (0.916 \pm 0.002)2\pi/a$, which agrees well with the value at $x = 0.05$ if it is corrected by the same enhancement shift as in pure Cr. It should be remembered, however, that temperature corrections to the band structure and susceptibility have not been considered in the present theoretical study.

Apparently, the only previous theoretical work on the role of alloying on the SDW is that of Machida and Fujita.[11] They obtained an exact solution to a mean-field Hamiltonian using a two-band, one-dimensional imperfect nesting model. The physical origin of their model is the Fermi-surface nesting that appears in Cr and was originally exploited by Lomer.[4] Their results for the concentration dependence of q_{SDW} are similar to those

presented here. The results reported here are derived using accurate band-structure and matrix elements in the calculation of the susceptibility. While approximations were made, the present work is a first-principles calculation which does not rely on empirical parameters for accurate comparison to experiment.

V. CONCLUSION

The unenhanced paramagnetic susceptibility of pure Cr has been computed within the random-phase approximation. At a wave-vector $q_{SDW} = 0.96(2\pi/a)$ along the Δ line there appears an antiferromagnetic instability towards an SDW ground state. The calculated q_{SDW} correlates well with Fermi-surface nesting features and is in very good agreement with neutron scattering measurements of the SDW wave vector. This result confirms that the role of Fermi-surface geometry is primary in the appearance of the SDW.

The calculation of the unenhanced susceptibility of pure Mo shows virtually no peak at the nesting vector despite the fact that the Fermi surface of Mo is very similar to that of Cr. This absence is due largely to matrix-element variation over the Brillouin zone. When many-body enhancements are included, this RPA peak is not sufficient to produce a pole in Mo.[19]

Dilute alloys of V or Mn in Cr also exhibit spin-density waves at wave vectors which vary with the concentration of impurity species. The computed concentration dependence of q_{SDW} for both V and Mn in Cr closely follow experimentally observed trends, further substantiating the long held belief in the relationship between paramagnetic Fermi-surface geometry and the spin-density-wave ground state of Cr and its alloys.

[1]W. C. Koehler, R. M. Moon, A. L. Trego, and A. R. Mackintosh, Phys. Rev. **151**, 405 (1966); see also references therein.

[2]A. W. Overhauser, Phys. Rev. Lett. **4**, 462 (1960); Phys. Rev. **128**, 1437 (1962).

[3]J. Callaway, A. K. Chatterjee, S. P. Singhal, and A. Ziegler, Phys. Rev. B **28**, 3818 (1983).

[4]W. M. Lomer, Proc. Phys. Soc., London **80**, 489 (1962); **84**, 327 (1964).

[5]P. C. Pattnaik, J. L. Fry, and N. E. Brener, J. Appl. Phys. **52**, 1646 (1981).

[6]E. Fawcett, Rev. Mod. Phys. **60**, 209 (1988).

[7]R. P. Gupta and S. K. Sinha, Phys. Rev. B **3**, 2401 (1971).

[8]C. G. Windsor, J. Phys. F **2**, 742 (1972).

[9]H. L. Skriver, J. Phys. F **11**, 19 (1981).

[10]J. Kubler, J. Magn. Magn. Mater. **20**, 277 (1980).

[11]K. Machida, Phys. Rev. B **30**, 418 (1984); K. Machida and M. Fujita, *ibid*. **30**, 5284 (1984).

[12]J. F. Janak, Phys. Rev. B **16**, 255 (1977).

[13]E. Clementi and C. Roetti, At. Data Nucl. Data Tables **14**, 277 (1974).

[14]G. Fletcher, J. L. Fry, P. C. Pattnaik, D. A. Papaconstantopoulos, and N. C. Bacalis, Phys. Rev. B **37**, 4944 (1988).

[15]W. A. Harrison, *Electronic Structure and the Properties of Solids* (Freeman, San Francisco, 1980).

[16]P. C. Pattnaik, P. H. Dickinson, and J. L. Fry, Phys. Rev. B **28**, 5281 (1983).

[17]D. G. Laurent, J. Callaway, J. L. Fry, and N. E. Brener, Phys. Rev. B **23**, 4977 (1981).

[18]J. Rath and A. J. Freeman, Phys. Rev. B **11**, 2109 (1975); P. C. Pattnaik, J. L. Fry, N. E. Brener, and G. Fletcher, Int. J. Quantum Chem. Symp. **15**, 499 (1981).

[19]J. L. Fry, Y. Z. Zhao, P. C. Pattnaik, V. L. Moruzzi, and D. A. Papaconstantopoulos, J. Appl. Phys. **63**, 4060 (1988); see also the discussion by E. Fawcett in Ref. 6 above.

[20]J. L. Fry, N. E. Brener, and R. K. Bruyere, Phys. Rev. B **16**, 5225 (1977).

[21]E. Fawcett, S. A. Werner, A. Goldman, and G. Shirane, Phys. Rev. Lett. **61**, 558 (1988).